Polarization and spin angular momentum in periodically rocking superlattice

Linghao Tian,[1] Kun Liu,[1,2] and Xianfeng Chen[1,3]

[1]Department of Physics; The State Key Laboratory on Fiber Optic Local Area Communication Networks and Advanced Optical Communication Systems, Shanghai Jiao Tong University, 800 Dongchuan Road Shanghai 200240, China

[2]e-mail: quenliu@sjtu.edu.cn

[3]e-mail: xfchen@sjtu.edu.cn

Received 16 March 2011; revised 3 July 2011; accepted 5 July 2011; posted 6 July 2011 (Doc. ID 143969); published 11 August 2011

The evolution of polarization and spin angular momentum (SAM) in periodically rocking superlattices (PRS) is investigated. Unlike in the birefringent crystal, they exhibit unusual properties. The evolution of polarization shows many remarkable trajectories and the SAM oscillates inside the PRS. The results may find applications in polarization-state or optical SAM control. © 2011 Optical Society of America

OCIS codes: 190.4400, 260.5430, 160.2100.

1. Introduction

The polarization state of the light that reflects the vector nature of the electromagnetic field is particularly striking when nonreciprocity comes into play and can have some far-reaching conceptual repercussions in applications [1]. As an old and fundamental issue, the management of polarization has triggered a growing interest due to the recent discovery of the optical spin Herr effect [2], which consists of the generation of a spin current, extremely promising for optical quantum-information processing [3]. Meanwhile, the spin angular momentum (SAM), which reflects the nature of the polarization state of a light, was demonstrated by Beth [4], and recent attempts have focused on the design of a handy SAM generator [5–7], which can play a significant role in the accurate manipulation in microscopic scale, such as particles and molecular in particular [8–10]. In this paper, we systematically studied the evolution of polarization and SAM of the light in a structure known as a periodically rocking superlattice (PRS). The results show that the evolution exhibits unusual properties. Diverse trajectories of the evolution of the polarization state with remarkable shapes were discovered. The evolution of SAM, which oscillates in the PRS, is also found to be distinctive. A critical wavelength is discovered in particular that separates the SAM of a light into two groups, with one containing more left-handed circularly polarized (LHCP) photons and the other more right-handed circularly polarized (RHCP) photons.

The material we discussed here is periodically poled lithium niobate (PPLN), a kind of nonlinear photonic crystal that has been widely investigated in many regions [11–14]. Previous studies have shown that PPLN can behave as a Solc-type rocking filter [15–17] when undergoing an external electric field, in which case the optical axis of the positive domain and the negative domain rotate a reversed small angle with respect to the optical plane of the input light, as shown in Fig. 1, and the modified PPLN is identified as the PRS. Here, we found that such PRS means more than a Solc-type rocking filter, as the rocking structure not only manipulates the intensity of a light but also performs a substantial impact on the polarization state of the light. Attractive devices on adaptive polarization control were made available with our recent attempts to manipulate the polarization state of the light coming out of a PRS via external electric field [18]. Here, we further our investigation on polarization evolution inside the

0003-6935/11/244728-05$15.00/0

PRS, and subsequently get an insight into the SAM of a light, which has not been fully understood.

2. Theoretical Analysis

A. Evolution of Polarization State

In a birefringent crystal, a polarized light decomposes into the ordinary wave (OW) and the extraordinary wave (EW), and the two waves, in general, do not exchange energy with each other. However, in PRS the rocking angle of the optical axis behaves as a periodical small perturbation, in which case the coupling of energy between OW and EW will be yielded. Considering $E_{1,2} = A_{1,2}(z) \times \exp[i(k_{1,2}z - \omega t)]$, the Jones vectors, which represent the polarization state of a light, can be given as a function of the distance inside the PRS by [19,20]

$$\vec{E}(z) = \begin{bmatrix} \{[\cos(sz) - i\Delta\beta/(2s)\sin(sz)]A_1(0) - i(\kappa/s)\sin(sz)A_2(0)\}e^{i\Delta\beta z/2} \\ \{(-i\kappa^*/s)\sin(sz)A_1(0) + [\cos(sz) + i\Delta\beta(/2s)\sin(sz)]A_2(0)\}e^{-i\Delta\beta z/2}e^{i(k_1-k_2)z} \end{bmatrix}, \tag{1}$$

with $\Delta\beta = (k_1 - k_2) - G_m$, $G_m = 2\pi m/\Lambda$, $\kappa = -\frac{\omega}{2c}\frac{n_o^2 n_e^2 \gamma_{51} E_y}{\sqrt{n_o n_e}}\frac{i(1-\cos m\pi)}{m\pi}$ $(m = 1, 3, 5\ldots)$, and $s^2 = \kappa\kappa^* + (\Delta\beta/2)^2$, where k_1 and k_2 are the corresponding wave vectors of OW and EW, G_m is the mth reciprocal vector corresponding to the periodicity of poling, Λ is the period of PPLN, n_o and n_e are the refractive indices of OW and EW, respectively; γ_{51} is the electro-optical coefficient, and E_y is the electric field intensity.

For a simplified case where the domain angle vanishes ($\kappa = 0$), Eq. (1) is hence derived as

$$\vec{E}(z) = \begin{bmatrix} A_1(0) \\ A_2(0)e^{i(k_1-k_2)z} \end{bmatrix}, \tag{2}$$

which describes the evolution of the polarization state in a birefringent crystal. The orthogonal circularly polarized modes A_+ and A_- can be obtained by means of the following relation:

$$\begin{cases} A_+ = (A_1 + iA_2)/\sqrt{2} \\ A_- = (A_1 - iA_2)/\sqrt{2} \end{cases}. \tag{3}$$

The polarization state is then determined by the complex ratio $\xi = A_+/A_-$, with the azimuth of the polarization ellipse being $\theta = 1/2\ \arg(\xi)$, where $\arg(\xi)$ takes the argument of a complex number, and the ellipticity is given by $e = (|\xi| - 1)/(|\xi| + 1)$.

The evolution of the polarization state of the light beam during propagation can be represented by a variety of graphic methods. Two particularly useful representations are the Poincare sphere [21] and the phase plane [22]. The latter was selected here to describe the evolution of the polarization state of a light. From Eq. (2) it is easy to see that the ellipticity and the azimuth of the polarization ellipse are oscillatory functions of distance along the propagation direction, with a period given by the beat length $L_0 = 2\pi/(k_1 - k_2)$. Starting from an arbitrary input polarization state, say $\theta = 30°, e = 0$, the polarization evolves with distance along a trajectory shown in Fig. 1(a), and the orbit closes after a distance equal to the beat length. Closed orbits represent oscillatory motions, which mean a polarized light will maintain its polarization state after a beat length.

The situation becomes significantly complicated in the PRS when $\kappa \neq 0$, in which case the periodical domain angle dramatically influences the evolution of the polarization state inside the crystal. For a simplified case when $\Delta\beta = 0$, Eq. (2) is derived as

$$\vec{E}(z) = \begin{bmatrix} A_1(0)\cos(|\kappa|z) - A_2(0)\sin(|\kappa|z) \\ \{A_2(0)\cos(|\kappa|z) + A_1(0)\sin(|\kappa|z)\}e^{i(k_1-k_2)z} \end{bmatrix}. \tag{4}$$

The beat length L_0 in this case is the minimum common multiple of $L_1 = 2\pi/(k_1 - k_2)$ and $L_2 = 2\pi/|\kappa|$. Starting from a linearly polarized light, for instance, $\theta = 0, e = 0$, the trajectory of evolution of the polarization under specific conditions ($L_2 = nL_1$, $n = 1, 2, 3$) are shown in Figs. 1(b)–1(d). Unlike in Fig. 1(a), where the evolution of polarization undergoes a single closed path, unusual multipaths are found when $\kappa \neq 0$. Besides, the number of the paths scales with n. Thus, the evolution of polarization can be controlled by adjusting the coupled coefficient κ, which is associated with the electric field intensity E_y. Likewise, when $\kappa \neq 0$, by adjusting external electric field and $\Delta\beta \neq 0$, by adjusting the operating wavelength, the beat length L_0 is the minimum common multiple of $L_1 = 2\pi/(k_1 - k_2)$, $L_2 = 2\pi/s$, and $L_3 = 2\pi/\Delta\beta$. In general, the magnitudes of L_1, L_2 and L_3 differ dramatically with each other, and the evolution of polarization splits into considerable discrete paths, which are shown in Figs. 1(e) and 1(f). In Fig. 1(e), an linearly polarized light, for instance, $\theta = 0$, $e = 0$, is incident, and the external electric filed is fixed at 8.5 kV/cm. In Fig. 1(f), an arbitrary input polarization state, say $\theta = 30°$, $e = 0$, is incident, and the external electric filed is fixed at 7.2 kV/cm. These discrete paths even develop into areas, covering more states of polarization than the case when $\Delta\beta = 0$ does.

B. Evolution of Spin Angular Momentum

Many studies have shown that light also carries angular momentum (AM). Generally, the AM of light

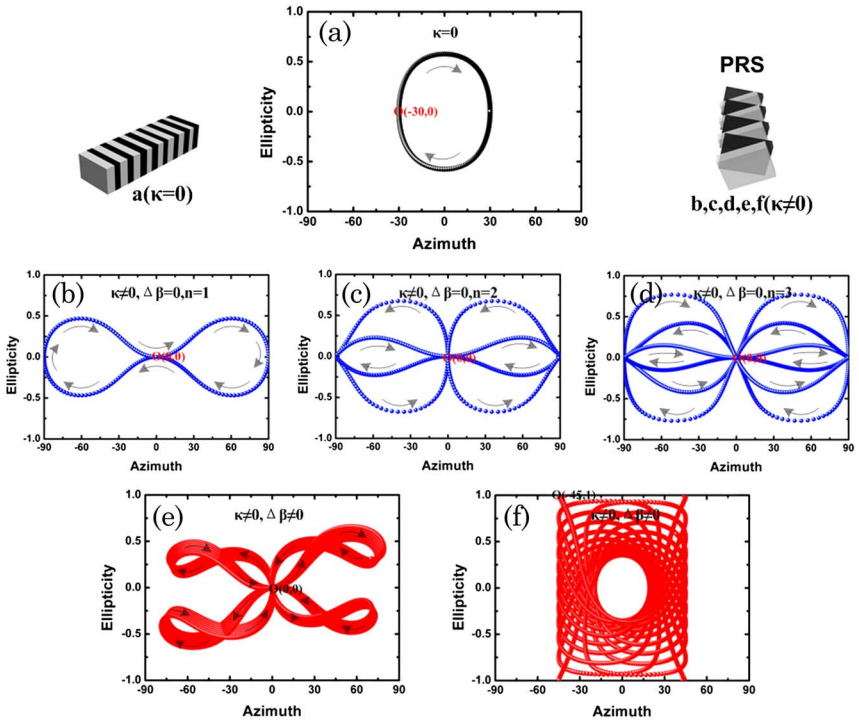

Fig. 1. (Color online) Phase-plane trajectories of the polarization state. (a), $\kappa = 0$ and the input state of polarization is $\theta = 30°$ and $e = 0$. (b)–(d), $\kappa \neq 0$, $\Delta\beta = 0$, and L_2 equals L_1, $2L_1$ and $3L_1$ for (b), (d) and (e), respectively, with the input state of polarization satisfying $\theta = 0$ and $e = 0$. (e), (f), $\kappa \neq 0$, $\Delta\beta \neq 0$. The initial state of polarization is $\theta = 0$, $e = 0$ for (e) and $\theta = -45°$, $e = 1$ for (f).

is separated into SAM and orbit AM, with the former determined by the polarization state of a light [4,23]. The control of SAM fundamentally aims at manipulating light and molecules, particles, or cells in the microscale and exploiting their interaction to create highly creative device in physical, chemical, biological, or medical science. As the evolution of polarization exhibits unusual characteristics in PRS, it is necessary to further investigate the behavior of SAM when light is propagating in it. When a monochromatic plane light with circular frequency ω is incident to the PPLN crystal along the X axis, it can be expressed as the superposition of LHCP and RHCP light:

$$\vec{E}(z) = \begin{bmatrix} E_1(z) \\ E_2(z) \end{bmatrix} = \left\{ E_{\text{lef}}(z) \begin{bmatrix} 1/\sqrt{2} \\ -i/\sqrt{2} \end{bmatrix} + E_{\text{rig}}(z) \begin{bmatrix} 1/\sqrt{2} \\ i/\sqrt{2} \end{bmatrix} \right\}. \quad (5)$$

According to the quantum theory, the energy of each photon is $\hbar\omega$, so the numbers of LHCP and RHCP photons transmitted at the output surface per unit area per second are respective average Poynting energy flow divided by $\hbar w$, i.e., $N_{\text{lef}}(z) = c\varepsilon_0|E_{\text{lef}}(z)|^2/2\hbar w$ and $N_{\text{rig}}(z) = c\varepsilon_0|E_{\text{rig}}(z)|^2/2\hbar w$. Each LHCP photon contains the AM of $\hbar$ and the RHCP one $-\hbar$. The total SAM is hence given by

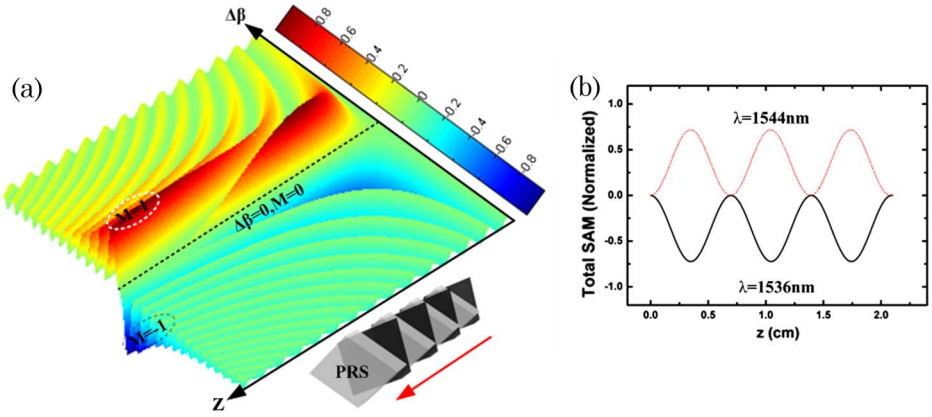

Fig. 2. (Color online) (a) shows the evolution of SAM inside the PRS for different phase mismatching conditions. The applied electric field is $E = 4\,\text{kV/cm}$; the wavelength ranges from 1520 nm to 1560 nm, and the wavelength that fulfills $\Delta\beta = 0$ is 1540 nm. Likewise, the temperature is 20 °C; (b) details the evolution of SAM with distance for wavelength at 1544 nm ($\Delta\beta > 0$) and 1536 nm ($\Delta\beta < 0$), respectively. It should be noted that the period of the PPLN is 21 μm, and the SAM inside the PRS is calculated every 21 μm started from the input port.

$$M(z) = \frac{c\varepsilon_0(|E_{\mathrm{lef}}(z)|^2 - |E_{\mathrm{rig}}(z)|^2)}{2w}. \quad (6)$$

Consider a simplified case, that is, $A_1(0) = 1$ and $A_2(0) = 0$. If $\kappa = 0$, we have $M(z) \equiv 0$. Otherwise, if $\kappa \neq 0$, the SAM oscillates in the PRS. Figure 2 presents the evolution of SAM inside the PRS. Three kinds of evolving behavior are identified: one is $M(z) \equiv 0$, when $\Delta\beta = 0$; one is $M(z) \geq 0$, when $\Delta\beta > 0$; and another is $M(z) \leq 0$, when $\Delta\beta < 0$. Here, the case $\Delta\beta = 0$ is a critical condition that separates the lights into two groups, with one ($\Delta\beta > 0$) consisting of more LHCP photons and the other ($\Delta\beta < 0$) consisting of more RHCP photons.

The SAM of lights with different wavelengths at a given distance ($z = 2.1$ cm) were also investigated and shown in Fig. 3(a). The period of the PPLN is 21 μm. At a temperature of 20 °C, the wavelength that satisfies $\Delta\beta = 0$ is calculated as 1540 nm by aid of semiller equation [24]. (a) indicates the normalized SAM can be transferred from −1 to 1 by adjusting the wavelength in the vicinity of the quasi-phase matched (QPM) condition ($\Delta\beta = 0$), which can behave as a controllable "spanner". Light with wavelength beyond 1540 nm can rotate a nanoscale particle clockwise, while light with wavelength below 1540 nm can exert an anticlockwise rotation on the particle. Thus, by modulating the wavelength from above 1540 nm to below 1540 nm, the normalized SAM oscillates from 1 to −1, and hence, a particle spins from clockwise to anticlockwise and with different AM. (a) also suggests the QPM condition can be detuned by temperature, and so does the SAM. About 2 °C is enough to realize the transfer of normalized SAM from 1 to −1. (b) shows the SAM is also modulated with the applied electric field when $\Delta\beta \neq 0$, and about 2 kV/cm is able to continuously completely transfer the SAM from $-\hbar$ to $\hbar$. Because the SAM can be controlled precisely by adjusting operating wavelength or temperature as discussed, it takes lots of convenience over the traditional method such as by rotating a 1/4 wave plate mechanically.

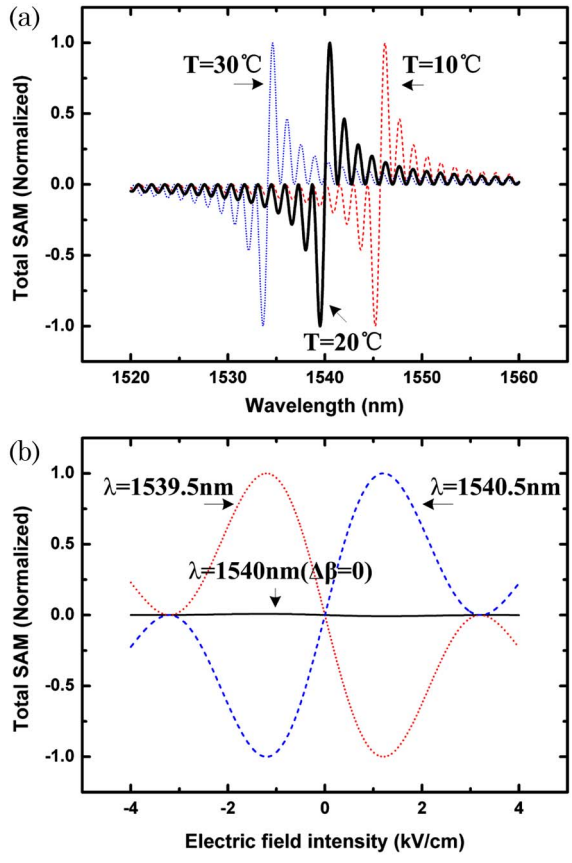

Fig. 3. (Color online) (a) shows the SAM of lights as a function of wavelengths at a given distance of 2.1 cm. Different temperatures of 10, 20 and 30 °C are considered. The applied electric field is $E = 1.2$ kV/cm. (b) shows the SAM of light as a function of the applied electric field. The distance is same 2.1 cm and the temperature is 20 °C. Different wavelengths of 1539.5 nm, 1540 nm and 1540.5 nm are studied.

3. Conclusion

In summary, the evolution of the polarization state and the SAM is studied in PRS. The results show that both the evolution of polarization and the evolution of SAM depend on the QPM condition. For cases when $\Delta\beta = 0$, the trajectories of polarization evolution undergo unusual multipaths rather than a single path happening in the bulk crystals. For cases when $\Delta\beta \neq 0$, the number of the paths is considerable and the trajectories even evolve into areas. Besides, when $\Delta\beta = 0$, the total SAM keeps zero but oscillates in the PRS when $\Delta\beta \neq 0$. The case $\Delta\beta = 0$ is also found to be a critical condition that separates the lights into two groups, with one ($\Delta\beta > 0$) consisting of more LHCP photons and the other ($\Delta\beta < 0$) consisting of more right-handed circularly photons. Furthermore, the distribution of SAM along wavelengths can be detuned by temperature and the SAM of a specific wavelength can be transferred from $-\hbar$ to $\hbar$ by adjusting applied electric field or temperature, promoting a straightforward method to manipulate the SAM of a light.

This research was supported by the National Natural Science Foundation of China (NFSC) No. 60508015 and No. 10574092, the National Basic Research Program "973" of China (2006CB806000), and the Shanghai Leading Academic Discipline Project (B201).

References

1. F. Jonsson and C. Flytzanis, "Polarization state controlled multistability of a nonlinear magneto-optic cavity," Phys. Rev. Lett. **82**, 1426–1429 (1999).
2. A. Kavokin, G. Malpuech, and M. Glazov, "Optical spin Hall effect," Phys. Rev. Lett. **95**, 136601 (2005).
3. C. Leyder, M. Romanelli, J. P. Karr, E. Giacobino, T. C. H. Liew, M. M. Glazov, A. V. Kavokin, G. Malpuech, and A. Bramati, "Observation of the optical spin Hall effect," Nat. Phys. **3**, 628–631 (2007).
4. R. A. Beth, "Mechanical detection and measurement of the angular momentum of light," Phys. Rev. **50**, 115–125 (1936).
5. L. X. Chen G. L. Zheng, J. Xu, B. Z. Zhang, and W. L. She, "Electrically controlled transfer of spin angular momentum

of light in an optically active medium," Opt. Lett. **31**, 3474–3476 (2006).
6. L. X. Chen, G. L. Zheng, and W. L. She, "Electrically and magnetically controlled optical spanner based on the transfer of spin angular momentum of light in an optically active medium," Phys. Rev. A **75**, 061403 (2007).
7. L. X. Chen and W. L. She, "Electro-optically forbidden or enhanced spin-to-orbital angular momentum conversion in a focused light beam," Opt. Lett. **33**, 696–698 (2008).
8. M. E. J. Friese, T. A. Nieminen, N. R. Heckenberg, and H. Rubinsztein-Dunlop, "Erratum: optical alignment and spinning of laser-trapped microscopic particles," Nature **395**, 621 (1998).
9. H. He, M. E. J. Friese, N. R. Heckenberg, and H. Rubinsztein-Dunlop, "Direct observation of transfer of angular momentum to absorptive particles from a laser beam with a phase singularity," Phys. Rev. Lett. **75**, 826–829 (1995).
10. B. Piccirillo, C. Toscano, F. Vetrano, and E. Santamato, "Orbital and spin photon angular momentum transfer in liquid crystals," Phys. Rev. Lett. **86**, 2285–2288 (2001).
11. V. Berger, "Nonlinear photonic crystals," Phys. Rev. Lett. **81**, 4136–4139 (1998).
12. S. N. Zhu, Y. Y. Zhu, and N. B. Ming, "Quasi-phase-matched third-harmonic generation in a quasi-periodic optical superlattice," Science **278**, 843–846 (1997).
13. S. N. Zhu, Y. Y. Zhu, Y. Q. Qin, H. F. Wang, C. Z. Ge, and N. B. Ming, "Experimental realization of second harmonic generation in a Fibonacci optical superlattice of $LiTaO_3$," Phys. Rev. Lett. **78**, 2752–2755 (1997).
14. Y. Y. Zhu, X. J. Zhang, Y. Q. Lu, Y. F. Chen, S. N. Zhu, and N. B. Ming, "New type of polariton in a piezoelectric superlattice," Phys. Rev. Lett. **90**, 053903 (2003).
15. X. F. Chen, J. H. Shi, Y. P. Chen, Y. M. Zhu, Y. X. Xia, and Y. L. Chen, "Electro-optic Solc-type wavelength filter in periodically poled lithium niobate," Opt. Lett. **28**, 2115–2117 (2003).
16. K. Liu, J. H. Shi, Z. E. Zhou, and X. F. Chen, "Electro-optic Solc-type flat-top bandpass filter based on periodically poled lithium niobate," Opt. Commun. **282**, 1207–1211 (2009).
17. K. Liu, J. H. Shi, and X. F. Chen, "Electro-optical flat-top bandpass Solc-type filter in periodically poled lithium niobate," Opt. Lett. **34**, 1051–1053 (2009).
18. K. Liu, J. H. Shi, and X. F. Chen, "Linear polarization-state generator with high precision in periodically poled lithium niobate," Appl. Phys. Lett. **94**, 101106 (2009).
19. P. Yeh, "Electromagnetic propagation in birefringent layered media," J. Opt. Soc. Am. **69**, 742–756 (1979).
20. Y. Q. Lu, Z. L. Wan, Q. Wang, Y. X. Xi, and N. B. Ming, "Electro-optic effect of periodically poled optical superlattice $LiNbO_3$ and its applications," Appl. Phys. Lett. **77**, 3719–3721 (2000).
21. R. Ulrich, "Representation of codirectional coupled waves," Opt. Lett. **1**, 109–111 (1977).
22. H. G. Winful, "Polarization instabilities in birefringent nonlinear media: application to fiber-optic devices," Opt. Lett. **11**, 33–35 (1986).
23. L. Allen, M. W. Beijersbergen, R. J. C. Spreeuw, and J. P. Woerdman, "Orbital angular momentum of light and the transformation of Laguerre-Gaussian laser modes," Phys. Rev. A **45**, 8185–8189 (1992).
24. D. H. Jundt, "Temperature-dependent Sellmeier equation for the index of refraction, no, in congruente lithium niobate," Opt. Lett. **22**, 1553–1555 (1997).